AUTHOR(S): WADDELL, S.A., FERNANDEZ, C., INVERARITY, C.C. and PRABHU, R.

TITLE: Extending the capability of forensic electrochemistry to the novel psychoactive substance benzylpiperazine.

YEAR: 2017

Publisher citation: WADDELL, S.A., FERNANDEZ, C., INVERARITY, C.C. and PRABHU, R. 2017. Extending the capability of forensic electrochemistry to the novel psychoactive substance benzylpiperazine. Sensing and bio-sensing research [online], 13, pages 28-39. Available from: https://doi.org/10.1016/j.sbsr.2016.12.001.

OpenAIR citation: WADDELL, S.A., FERNANDEZ, C., INVERARITY, C.C. and PRABHU, R. 2017. Extending the capability of forensic electrochemistry to the novel psychoactive substance benzylpiperazine. Sensing and bio-sensing research, 13, pages 28-39. Held on OpenAIR [online]. Available from: https://openair.org.ac.uk.

Sensing and Bio-Sensing Research 13 (2017) 28–39

Contents lists available at ScienceDirect

Sensing and Bio-Sensing Research

journal homepage: www.elsevier.com/locate/sbsr

Extending the capability of forensic electrochemistry to the novel psychoactive substance benzylpiperazine

S.A. Waddell [a,*], C. Fernandez [a], C.C. Inverarity [a], R. Prabhu [b]

[a] School of Pharmacy and Life Sciences, Robert Gordon University, Garthdee Road, Aberdeen AB10 7GJ, United Kingdom
[b] School of Engineering, Robert Gordon University, Garthdee Road, Aberdeen AB10 7GJ, United Kingdom

ARTICLE INFO

Article history:
Received 8 July 2016
Received in revised form 9 December 2016
Accepted 16 December 2016
Available online xxxx

Keywords:
Voltammetry
Forensic
Controlled drugs
Benzylpiperazine
Ecstasy

ABSTRACT

Benzylpiperazine (BZP) is a novel psychoactive substance that is commonly abused in tablet form as an "ecstasy-type" drug. Electroanalysis offers genuine potential for field testing of bulk drug samples. This research is the first to investigate the viability of voltammetric analysis of BZP. Initial cyclic voltammetry in 0.1 M KCl showed an oxidative peak at a glassy carbon electrode for BZP at approximately 0.8 V (scan rate 205 mV s^{-1}). Next an optimised electrode/electrolyte combination (viz. 80:20 W:W glassy carbon beads:nujol and pH 9.5, 40 mM, Britton-Robinson buffer) was developed using $K_3Fe(CN)_6$ to test the electrode material. The oxidation of BZP involves two electrons and two protons and a mechanism has been proposed. An anodic stripping square wave voltammetric method was optimised by factorial design with the conditions of deposition: −0.8 V for 135 s, and stripping: step height 10 mV, amplitude 50 mV and frequency 13 Hz. A limit of detection of 6 μM was achieved. The resolution against 3,4-methylenedioxymethylamphetamine (MDMA) was also verified.

1. Introduction

The abuse of ecstasy tablets came to prominence across Europe during the late 1980′s at which time the major active ingredient was 3,4-methylenedioxymethylamphetamine (MDMA) [1]. However over the years clandestine laboratories have sought to circumvent the law by producing tablets containing compounds which were not under control. This has led to an enormous range of compounds being seized worldwide. In fact, the 2015 World Drugs Report estimates 500 compounds are abused globally [2]. In order to deal with such a vast issue the United Kingdom introduced the Psychoactive Substances Act 2016 wherein such a substance was defined as that which "produces a psychoactive effect in a person if, by stimulating or depressing the person's central nervous system, it affects the person's mental functioning or emotional state" [3]. Although the substances are defined by their action rather than their structure, there are broad families of compounds which are commonly encountered namely: aminoindanes, synthetic cannabinoids, cathinones, ketamine and phencyclidine-types, phenethylamines, piperazines and tryptamines [4]. Further to this, the generality of the terminology in the legislation enables law enforcement to seize any New Psychoactive Substances (NPSs), as they are commonly known, resulting in a wide array of compounds which are presented for analysis to forensic agencies. An excellent overview which outlines the recent analytical strategies undertaken is given by Smith et al. [5].

Benzylpiperazine (BZP) is one such NPS, structure shown in Fig. 1. The importance of BZP in Europe was first noted in the early part of the 21st century as it was being sold as a "legal high" over the internet [6]. There was also some confusion at the time with piperazines being sold as "herbal highs" although they are entirely synthetic. This may have been due to structural similarities with the pepper derived compound piperidine [7]. Then in 2009 the European Monitoring Centre for Drugs and Drug Addiction (EMCDDA) advised that the member states should control BZP stating: "due to its stimulant properties, risk to health, the lack of medical benefits and following the precautionary principle, there is a need to control BZP, but the control measures should be appropriate to the relatively low risks of the substance" [8]. In the UK, BZP and structurally related analogues were brought under control of the Misuse of Drugs Act 1971, being listed as Class C in 2009 [9].

There already exists a wide array of chromatographic analytical methodologies in the scientific literature regarding the analysis of BZP. A brief synthesis of the analysis of BZP in a range of matrices is shown in Table 1. Typical limits of detection (LOD) tend to be in the nanomolar range, and this is indeed necessary for the analysis

* Corresponding author.
E-mail address: s.waddell1@rgu.ac.uk (S.A. Waddell).

http://dx.doi.org/10.1016/j.sbsr.2016.12.001

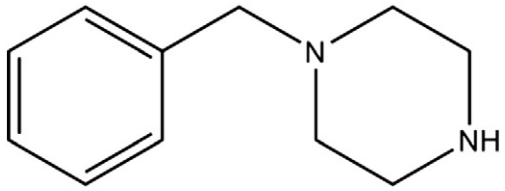

Fig. 1. Structure of benzylpiperazine (BZP).

of clinical samples and wastewater, however it should also be noted that the methods are normally accompanied by a prior extraction step in order to attain LOD values in this range. It is also noteworthy that expensive, lab based instrumentation is required for this type of analysis which makes it unsuitable for field testing of bulk drugs.

Consequently a number of presumptive tests have been developed that can detect the presence of BZP. One such novel presumptive spot test was developed by Philp et al. [10] using sodium 1,2-naphthoquinone-4-sulphonate to produce a dark red colour for BZP. The proposed reaction scheme for this test is shown in Fig. 2. They subjected the test to rigorous validation against many active ingredients and excipients commonly found in ecstasy-type seizures and were also able to determine an LOD of 40 μg, which is more than sensitive enough for its purpose. Piperidine has long been known to be a precursor for phencyclidine [11] and as such has been monitored closely. In a United Nations Scientific and Technical Note the formation of a blue-coloured Simon-Awe complex is described, as shown in Fig. 3 [12]. Almost all piperazines contain the same active moiety as piperidine and as such this general test for secondary amines could be applied. It is in fact the amine functionality that enables colorimetric detection for all the common presumptive tests [6].

Microcrystalline identification does not offer as low an LOD as the colorimetric spot tests, but the growing habits that are observed between reagents and drugs can be very specific [13]. Elie et al. [14] designed a microcrystalline assay for BZP using mercury chloride as the reagent. Upon gentle mechanical assistance for nucleation, BZP was found to form distinctive rectangular plates.

Table 1
Chromatographic analytical methodologies for the analysis of BZP.

Matrix	Extraction and derivatisation	Analytical conditions	Limit of detection	Reference
Urine	Enzymatic hydrolysis with 100 mM acetate buffer containing sulfatase/β-glucuronidase, then solid phase extraction with Oasis HLB	Liquid Chromatography: SCX column (150 mm × 2 mm); 40 mM pH 4 Acetate Buffer:MeCN 25:75 v:v at 0.15 mL min^{-1}; Shimadzu LCMS 2010A mass analyser	30 nM	[33]
		Gas Chromatography: DB-5MS column (30 m × 0.25 mm × 0.25 μm); He 1.0 mL min^{-1}; Shimadzu GCMS QP-2010 mass analyser	300 nM	
Tablets and capsules	10 min ultrasonication in 20 mM HCl:MeOH 1:1 v:v	Liquid Chromatography: L-column ODS or SymmetryShield R_{18} (150 mm × 4.6 mm × 5 μm); 10 mM SDS in MeCN:H_2O:H_3PO_4 300:700:1 v:v:v at 1 mL min^{-1}; Diode array detector at 199–360 nm	Not given	[34]
		Gas Chromatography: DB-5MS column (30 m × 0.25 mm × 0.25 μm); He 1.1 mL min^{-1}; Agilent N3520 mass analyser	Not given	
Plasma and urine	Centrifugation then deproteinized with 35% $ZnSO_4$ plus enzymatic hydrolysis of urine	Liquid Chromatography: Zorbax C18 column (150 mm × 4.6 mm × 5 μm); gradient using 0.01 M pH 4.5 NH_4CHOO and MeCN at 1 mL min^{-1}; Agilent MSD model D single stage quadrupole mass analyser	30 nM	[35]
Plasma	Dilution with pH 6 Phosphate buffer then solid phase extraction using Chromabond Drug	Liquid Chromatography: Synergi Polar RP column (150 mm × 2 mm × 4 μm); gradient using 0.1% CHOOH in 1 mM NH_4CHOO and 0.1% CHOOH in MeOH at 0.25 mL min^{-1}; Sciex API 365 tandem mass analyser	30 nM	[36]
Simulated Wastewater	Filtration the SPE using XRDAH506	Liquid Chromatography: Luna pentafluorophenyl column (50 mm × 4.6 mm × 3 μm); gradient using MeOH and 0.1% CHOOH at 0.5 mL min^{-1}; AB Sciex Q-Trap mass analyser	6 pM	[37]
Simulated tablets	Dilution only for liquid chromatography and heptafluorobutyric acid derivatisation and silylation using SilPrep for gas chromatography	Liquid Chromatography: Hypersil C18 column (125 mm × 3 mm × 3 μm); gradient using pH 3.2 PB and MeCN at 0.4 mL min^{-1}; DAD at 210 to 400 nm	50 μM	[38]
		Gas Chromatography: heptafluorobutyric acid derivatisation and silylation using SilPrep®; HP-5MS column (30 m × 0.25 mm × 0.25 μm); He 1.0 mL min^{-1}; Agilent 5971A mass analyser	3 μM	
Urine	Liquid/liquid extraction using KOH	Gas Chromatography: pentafluoropropionic anhydride derivatisation; J&W column (20 m × 0.18 mm × 0.18 μm); He 1.0 mL min^{-1}; Agilent 5975 mass analyser	150 nM	[39]
Urine	Centrifugation then solid phase extraction using SOLA SCX	Liquid Chromatography: Accucore C18 (100 mm × 2.1 mm × 2.6 μm); gradient elution using 0.1% HCOOH in water and 0.1% HCOOH in MeCN at 0.4 mL min^{-1}; Thermo Scientific NCS-3500RS UltiMate 3000 Binary Rapid system coupled to a Thermo Scientific Q Exactive Mass spectrometer	6 nM	[40]
Hair	Overnight sonication in 0.1% HCOOH	Liquid Chromatography: Kinetex C18 column (100 × 2.1 mm × 2.6 μm); gradient elution using 0.1% HCOOH in 5 mM NH_4HCOO and 0.1% HCOOH in 1:1 v:v MeOH: MeCN at 0.35 mL min^{-1}; Agilent 6460 triple quadrupole mass spectrometer	5 pg/mg of hair	[41]
Tablets	Dissolution in water then freeze dried overnight	Liquid Chromatography: Synergi Hydro-RP Phenomenex column (250 mm × 10 mm); gradient elution using 0.05% CF_3COOH in water and MeCN at 3 mL min^{-1}; UV detection at 208 nm	Not given	[42]
		Gas Chromatography: DB1-ms column (15 m × 0.25 mm × 0.25 pm sic); He 2 mL min^{-1}; Agilent 5975C MSD Series with a Triple-Axis Detector	Not given	
Tablets	Unltrasonication in 2-methyl-propan-2-ol then centrifugation	Gas Chromatography: Supelco Equity 5 column (30 m × 0.25 mm × 0.25 μm); He 1 mL min^{-1}; Perkin Elmer Clarus Turbomass Gold 500MS detector.	2 nM	[43]
Wastewater	Solid phase extraction using Oasis MCX.	Gas Chromatography: Pentafluoropropionic anhydride derivatisation; Supelco Equity TM-5 column (30 m × 0.25 mm × 0.25 μm); He 1 mL min^{-1}; PerkinElmer Clarus 500 Gas Chromatograph-Mass Spectrometer detector	0.14 pg on column	[44]

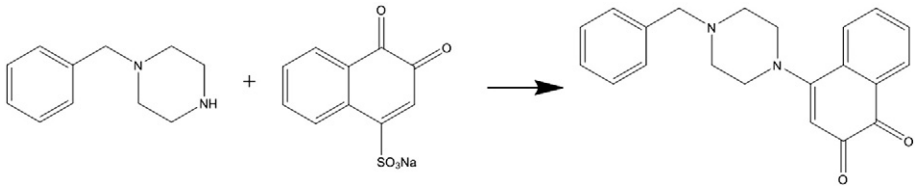

Fig. 2. Reaction scheme for the BZP presumptive colour test which uses 1,2-naphthoquinone [7].

BZP is known to produce psychomotor effects similar to amphetamine [15]. Notwithstanding BZP acting on the same receptors as amphetamine, it may not bind to the same antibodies as those used in amphetamine immunoassays. The response of several piperazines was checked against an enzyme-multiple immunoassay technique (EMIT) and a fluorescence polarisation immunoassay (FPIA) initially designed for amphetamine and methylamphetamine [16]. The FPIA did not detect BZP in a 100,000 ng mL^{-1} spiked urine sample. However the amphetamine EMIT did respond to BZP with cross reactivities of 0.4% and 1.3% at 300 and 12,000 ng mL^{-1} amphetamine equivalents respectively. There are currently no commercially available immunoassays specifically for piperazines [6], however some recent literature has been published to this effect [17]. Also in general with presumptive testing false positives are possible [18] and they are at best semi-quantitative [19].

There can be no doubt as to the general reliability of electrochemical measurements in light of the facts that: globally amperometric quantitation of glucose is relied upon by millions of diabetes patients [20], there is widespread use of fuel-cell breath-alcohol testers by police forces [21] amongst many other medical applications [22]. The major advantages of electrochemical analysis over other techniques can be summarised as:

- Miniaturisation enables portability and the analysis of samples of very small volume [23].
- Through proper electrode design a high level of sensitivity, selectivity and stability can be achieved [24].
- The analysis is generally faster and simpler than other techniques [25].
- It is far cheaper than most other techniques with comparable limits of quantification (LOQ) [26].

These benefits could of course be useful in field testing in a forensic context and indeed the relatively new field of "forensic electrochemistry" has found a range of applications in recent years [27] including the voltammetric analysis of gunshot residue using an innovative "lab-on-a-finger" technique [28], and explosives [28]. However the bulk of the published forensic electrochemistry research lies in the area of drug analysis. Some recent highlights from this are presented in Table 2.

It was the aim of this research to assess the viability of voltammetric analysis of BZP as the technique lends itself so well to potential field use. This research comprises the first time the voltammetric analysis of BZP has been reported.

2. Experimental

2.1. Materials

All voltammetric analysis was carried out using a PGStat128N potentiostat in combination with the NOVA software v1.11 (both Metrohm Autolab). An Ag|AgCl reference electrode and a Pt sheet counter electrode were used for all analysis (both Metrohm Autolab). A 2 mm diameter graphite electrode (Metrohm Autolab), a 2 mm diameter gold and a 2 mm diameter platinum electrode (both BASi) were cleaned with an aqueous slurry using 15 μm alumina (Microabrasives Corp.) then sonicated in de-ionised water for 60 s prior to use as the solid working electrodes for the initial investigation. Three carbon powders of different particle sizes (all Aldrich) and Nujol (Plough UK) were used to form the paste electrodes. The respective ratios of carbon and nujol were triturated for 20 min in a pestle and mortar prior to being housed in a Teflon electrode (BASi) with a 3 mm exposed area. A Zeiss EVO LS scanning electron microscope (SEM) was used to capture images of the carbon powders. The chemicals used in the preparation of the background electrolytes were all laboratory reagent grade (Fischer Scientific) and used without any further purification. Background electrolytes were thoroughly degassed by nitrogen bubbling. The potassium ferricyanide was a laboratory reagent of 99% purity. A liquid BZP standard of purity ≥90% (Bione) was used for the analysis with the solid electrodes and a BZP hydrochloride salt, ≥98% (Cayman Chemicals) was used in the analysis using the paste electrodes. A 3,4-methylenedioxymethylamphetamine (MDMA) hydrochloride salt standard of purity ≥98% (Sigma) was used to assess the selectivity of the method. All drug concentrations are reported as base rather than as the salt. Deionised water with a resistivity of 18.2 MΩ cm was used to prepare the solutions. The software Minitab v16 (Minitab Inc.) was used to produce and analyse the factorial design experiment.

2.2. Initial investigation

A 10 mL cell volume of approximately 50 μM BZP in 0.1 M KCl was prepared and cyclic voltammograms (CVs) were run using the solid graphite, gold and platinum electrodes and each was checked against an appropriate blank. Five scans in total were taken for each cell using a scan rate (υ) of 250 mV s^{-1} and a step height of 2.4 mV.

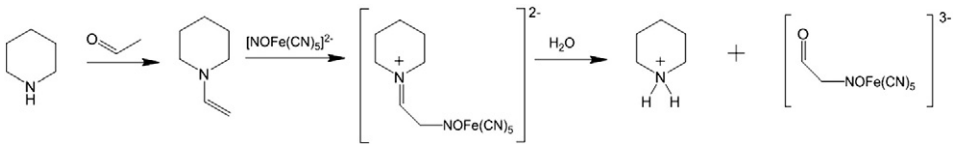

Fig. 3. Reaction scheme for the United Nations piperidine colour test [9].

Table 2
Recent voltammetric controlled drug research. New acronyms in table: WE working electrode; THF tetrahydrofuran; HMDE hanging mercury drop electrode; BR Britton Robinson buffer; AdSDPV adsorptive stripping differential pulsed voltammetry; GCE glassy carbon electrode; CV cyclic voltammetry; OCP open circuit potential; SCE saturated calomel electrode; LSV linear sweep voltammetry; AdSSWV adsorptive stripping square wave voltammetry; SWV square wave voltammetry; ITO indium tin oxide; SAM self assembled monolayers; MWCNT multiwalled carbon nanotubes.

Analyte/s and (matrix)	Extraction	WE and (technique)	Analytical conditions	LOD (ng mL^{-1})	Ref
Morphine and noscapine (plasma)	Centrifuged and vortexed with 0.7 M $ZnSO_4$, bicarbonate and THF	HMDE (AdSDPV)	BR pH 10; deposition at -100 mV vs. Ag|AgCl for 150 s, then stripped from 100 to 400 mV at 40 mVs^{-1} with amplitude 100 mV	morphine 3 noscapine 7	[45]
Morphine (urine)	Dilution only	GCE (CV)	50 mM PB at pH 7.4; stirred accumulation at OCP for 90s, then CV from 0 to 700 mV vs. Ag|AgCl at 100 mV s^{-1}	57	[46]
MDMA (standards only)	–	GCE (CV)	50 mM PB at pH 7.4; scanned 1000 to −500 mV vs. SCE	–	[47]
Cocaine (powder)	Dilution only	PDE modified with cobalt hexacyanoferrate (LSV)	0.1 M $NaClO_4$ in MeCN; 0 to 1200 mV at 100 mV s^{-1} vs. Ag|AgCl	43	[48]
Zopiclone (urine and Imovane® tablets)	Tablets were crushed and centrifuged in H_2O	GCE (AdSSWV)	BR pH 7.08; deposition at 600 mV vs. Ag|AgCl for 120 s, then stripped from 200 to 1400 mV with amplitude 50 mV, frequency 50 Hz and step 10 mV.	66	[49]
Clonazepam, flurazepam, alprazolam, midazolam, medazepam, chlordiazepoxide and diazepam (phytotherapeutic formulations)	Dilution in MeOH	HMDE (AdSDPV)	Ringer buffer pH 10.0; 10 s deposition at varying potential depending on analyte from −400 to −800 mV vs. Ag|AgCl and subsequent varying sweeps, using pulse amplitude -50 mV, pulse duration 40 ms, scan rate 50 mV s^{-1}	–	[50]
Amphetamine, MEA, MDA, MDMA (serum and tablets)	Tablets sonicated for 5 min in H_2O and filtered. MeOH added to serum then vortexed and centrifuged	GCE (SWV)	0.2 M PB pH 7; scan 0 to 1500 mV vs. Ag|AgCl with frequency 100 Hz and pulse amplitude 50 mV	MDMA 464	[51]
Morphine (standards only)	–	ITO modified with poly(3,4-ethyleenedioxythiophene) and further activated with IrO2 (LSV)	0.5 M sulphate buffer pH 2; scan 0 to 1300 mV vs. Ag|AgCl at 50 m V s^{-1}	–	[52]
Cocaine (standards only)	–	ITO modified by SAM of ferrocene and Au nanoparticles and activated with cocaine aptamer fragment SH-C2 (DPV)	0.1 M PB pH 6.5; scan 700 to 0 mV vs. Ag|AgCl with modulation time 50 ms, interval time 0.5 s, modulation amplitude 25 mV and potential step 5 mV.	30	[53]
Morphine (urine)	Centrifuged and diluted with PB pH 8.0	MCPE using graphite: MWCNT 4:1 w:w in paraffin oil with 1-butyl-3-methylimidazolium hexafluoro phosphate binder (DPV)	0.1 M PB pH 8.0; scan 100 to 600 mV vs. Ag|AgCl with pulse height 100 mV and pulse width 5 mV.	40	[54]
Morphine (serum)	Dilution only	GCE modified with Au nanotube array on an anodic aluminium oxide template (DPV)	0.1 M phosphate and citric acid buffer pH 6.1; other parameters not specified	12	[55]
MCPE modified carbon paste electrode; HRP horseradish peroxidase; THC Δ^9-tetrahydrocannabinol					
Cocaine (serum)	Dilution with 10 mM PB pH 7.4 and 1 M NaCl	Au electrode modified by tetrahedron SAM of thiolated aptamers (Chronoamperometry)	Cocaine fuses the aptamers aca-1 and biotinylated aca-2. This is followed by the binding of avidin-HRP conjugates to aca-2′s biotin tag. As HRP can now act as a catalyst for H_2O_2 reduction in the presence of 3,3′,5,5′-tetramethylbenzidine an amperometric signal is produced	10	[56]
Codeine (tablets)	Crushed and dissolved in 0.2 M AB pH 4.5	GCE (SWV)	0.2 M AB pH 4.5; scan 0 to 1800 mV vs. Ag|AgCl with frequency 75 Hz, amplitude 50 mV and increment 5 mV	761	[57]
Morphine (urine)	Dilution only	MCPE using electrodeposition of ferrocene and Au nanoparticles (DPV)	0.04 M BR pH 7.4; scan 100 to 600 mV vs. Ag|AgCl with scan rate 10 mV s^{-1} pulse width 25 ms, pulse period 200 ms and pulse amplitude 10 mV	1	[58]
Morphine (urine)	Centrifuged and diluted with PB pH 7.0	MCPE using graphite:MWCNT: n-hexyl-3-methylimidazolium hexafluorophosphate 64.5:15.5:20 w:w:w in paraffin oil (DPV)	0.1 M PB pH 7.0; scan 300 to 600 mV vs. Ag|AgCl with pulse height 80 mV and pulse width 7 mV	6	[59]
THC (hemp and hashish)	10 min US in MeOH then filtered. Filtrate then subject to preparative TLC	GCE (LSV)	0.1 M tetrabutylammonium tetrafluoroborate in *N*,*N*-dimethylformamide:H_2O 9:1 v:v; 30s deposition at −1200 mV vs. Ag|AgCl then scan −1000 to 500 mV at 100 mV s^{-1}	0.34	[60]
Morphine (urine and pharmaceutical formulations)	Urine was filtered prior to dilution in 0.15 PB pH 7.0	MCPE using graphite:MWCNT:4-hydroxy-2-(triphenylphosphino)phenolate 200:2:1 w:w:w in paraffin oil	0.15 M PB pH 7.0; other parameters not specified	19	[61]

(continued on next page)

Table 2 (*continued*)

Analyte/s and (matrix)	Extraction	WE and (technique)	Analytical conditions	LOD ($ng\ mL^{-1}$)	Ref
		(DPV)			
Morphine, noscapine and diamorphine (standards only)	–	GCE modified with graphene nanosheets (DPV)	0.1 M PB pH 8.0; scan from 100 to 1100 mV vs. Ag|AgCl with voltage step 8 mV, scan rate 20 mV s^{-1} and pulse amplitude 50 mV	morphine 114 noscapine 83 diamorphine 185	[62]
Morphine (standards only)	–	Au electrode by SAM of 2-aminoethanethiol (CV)	0.2 M PB pH 6.0; scan 0 to 800 mV vs. Ag|AgCl at a range of scan rates	–	[63]
Morphine (urine)	Dilution only	MCPE using graphite:Al_2O_3 nanoparticles 9:1 w:w in paraffin oil (SWV)	0.1 M PB pH 7.0; other parameters not specified	9	[64]
GHB (standards only)	–	Pt (CV)	0.1 M $HClO_4$ and 0.1 M H_3PO_4; scan −200 to 1200 mV vs. Ag|AgCl at 10 mV s^{-1}	–	[65]
Codeine (urine)	Centrifuged and diluted with PB pH 4.0	GCE modified with graphene and Nafion (SWV)	0.1 M PBS pH 4.0; stirred accumulation at OCP for 180 s then scan 700 to 1300 mV using amplitude 50 mV, step height 6 mV and frequency 12 Hz	5	[66]
Cocaine (standards only)	–	Pt electrode modified with [UO_2(*N*,*N*′-Ethylenebis(3-methoxysalicylideneaminato))(H_2O)]·H_2O (CV)	1 M KCl and 0.001 M HCl; scan −300 to 400 mV vs. Ag|AgCl at 100 mV s^{-1}	21	[67]
New acronyms in table: GHB γ-hydroxybutyric acid; PBS phosphate buffered saline; CPE carbon paste electrode; SDS sodium dodecyl sulphate					
Buprenorphine (urine)	Dilution only	CPE (DPV)	0.24 mM SDS in 0.2 M PB pH 3.0; stirred accumulation at OCP for 120 s then scan 300 to 1000 mV with pulse height 10 mV and scan rate 90 mV s^{-1}	7	[68]
Morphine (urine and pharmaceutical samples)	Centrifuged and filtered prior to dilution	MCPE using graphite: NiO modified MWCNT: 1-methyl-3-butylimidazolium chloride 70:35:25 w:w:w in paraffin oil (SWV)	0.1 M PB pH 7.0; other parameters not specified	3	[69]
Morphine (serum and urine)	Dilution only	GCE modified with electrochemically reduced MWCNT graphene oxide (LSV)	0.1 M PB pH 4.5; stirred accumulation at OCP for 120 s then scan 200 to 900 mV at 100 mV s^{-1}	14	[70]
Morphine (urine)	Supported liquid membrane extraction using 2-nitrophenyl octyl ether containing 10% tris-(2-ethylhexyl) phosphate and 10% di-(2-ethylhexyl) phosphate	Carbon SPE (DPV)	0.1 M NaOH; scan 0 to 600 mV vs. Ag pseudoreference with step 15 mV and pulse amplitude 50 mV	2	[71]
Methadone (urine and saliva)	MeCN was added to urine then all samples were vortexed and centrifuged	MCPE using graphite:MWCNT 65:10 w:w then electrodeposition of Au nanoparticles (AdSSWV)	0.04 M BR pH 9.0; deposition at 700 mV vs. Ag|AgCl for 100 s then scan 500 to 1250 mV with pulse amplitude 100 mV and frequency 25 Hz	5	[72]
Cocaine (powder)	Dilution only	Carbon SPE modified with MWCNT (SWV)	0.1 M PBS pH 10; scan 0 to 1500 mV vs Ag|AgCl with step potential 12 mV, frequency 25 Hz and amplitude 25 mV	–	[72]
MDMA (Standards only)	–	GCE modified with Nafion and cucurbit[6]uril (CV)	KCl solution; scan 800 to 1300 mV at 100 mV s^{-1}	3	[73]
Methcathinone, mephedrone and 4-MEC (standards only)	–	Carbon SPE (CV)	PB pH 2; scan 0 to 1700 mV vs. SCE at 100 mV s^{-1}	methcathinone 44500 mephedrone 39800 4-MEC 84200	[30]
Morphine (serum)	MeCN was added to serum then samples were vortexed and centrifuged	GCE modified with Nafion and MWCNT (AdSSWV)	0.1 M H_2SO_4; deposition at -500 mV vs. Ag|AgCl for 360 s then scan 700 to 1400 mV with potential step 8 mV, frequency 75 Hz and amplitude 25 mV	9	[74]
Morphine and codeine (serum and urine)	Urine was centrifuged and filtered. Serum had 20% v:v $HClO_4$ added, vortexed then centrifuged	Pencil graphite electrode modified with PDDA and aptamers (AdSDPV)	0.1 M PB pH 7.0; stirred accumulation at OCP for 300 s then scan from 0 to 900 mV with pulse amplitude 50 mV, modulation time 0.05 s and step potential 8 mV	morphine 41 codeine 43	[75]

2.3. Carbon paste electrode development

In order to investigate the effects of particle size, allotrope, and organic binder, three different forms of carbon powder were each mixed in two different ratios with nujol as shown in Table 3. Although this study is not exhaustive, its reduced form does permit a comparison between graphite and glassy carbon alongside a threefold difference in particle size. SEM images of the three carbon powders were captured using the secondary electron detector under high vacuum with a working distance of 10 mm and an anode potential of 25 kV. A 10 mM

Table 3
Ratios of carbon to nujol used in assessment of paste electrodes.

Paste number	Allotrope of carbon	Particle size (μm)	Carbon (%W/W)	Nujol (%W/W)
1	Graphite	<45	60	40
2	Graphite	<45	80	20
3	Graphite	<150	60	40
4	Graphite	<150	80	20
5	Glassy carbon	2–12	60	40
6	Glassy carbon	2–12	80	20

Table 4
Factorial design for optimisation of square wave voltammetry of BZP using Paste 6.

Run order	Step (mV)	Amplitude (mV)	Frequency (Hz)
1	10	5	5
2	1	5	50
3	10	5	50
4	1	50	5
5	10	50	50
6	1	5	5
7	1	50	50
8	10	50	5

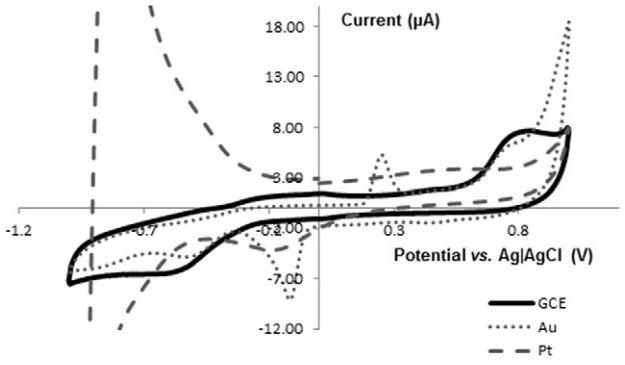

Fig. 4. CV of 50 μM BZP using graphite (GCE), gold (Au) and platinum (Pt) electrodes. The second scan of five is shown in each case and platinum is shown as off scale for clarity of the important oxidative peaks ($\upsilon = 250$ mV s^{-1}).

$K_3Fe(CN)_6$ solution was prepared in 0.1 M KCl as a spiking solution for standard addition analysis by square wave voltammetry (SWV). The concentration range 99 to 909 μM of $K_3Fe(CN)_6$ in 0.1 M KCl was tested for each paste electrode using the voltage program deposition at −0.5 V for 30 s then stripping up to 1.0 V with a step of 5 mV, amplitude of 20 mV and a frequency of 25 Hz. Three CVs were also obtained for the 99 μM of $K_3Fe(CN)_6$ cell using three scan rates: 10, 100 and 500 mV s^{-1}. The particular study was limited to three different rates as it was not deemed necessary to examine the $[Fe(CN)_6]^{3-/2-}$ redox process in detail. It was however deemed informative to gain values for the slope of the Randles-Sevcik plot for each paste for comparison. In each CV the working electrode potential started at 0.0 V and was swept to 1.0 V then cycled between −0.7 V and 1.0 V a total of 3 times with a step of 2.4 mV.

2.4. Mechanism investigation

Seven separate Britton-Robinson (BR) buffers at 40 mM were prepared to cover the pH range 4 to 10. These were used as the background electrolyte for 49 μM BZP cells. Each pH cell was investigated by linear sweep voltammetry (LSV) using the Paste 6 working electrode from −0.8 V to 1.0 V with a scan rate of 500 mV s^{-1} and step of 2.4 mV. A further BR buffer at pH 9.5 was also prepared as the background electrolyte for a 67 μm BZP solution in order to assess the LSV over the same potential range but with varying scan rates of 10, 25, 50, 100, 250, and 500 mV s^{-1} using the Paste 6 electrode.

2.5. Method development

A 100 μM BZP was prepared in pH 9.5 BR buffer and analysed by SWV using the Paste 6 electrode. Increasing levels of deposition time were tested in order to assess when electrode saturation occurred. Otherwise the working electrode was swept from −0.8 V to 1.0 V with a step of 5 mV, and amplitude of 20 mV and a frequency of 25 Hz. Once the best deposition time was determined the SWV was further optimised with the same cell using a factorial design as shown in Table 4.

2.6. Method validation

The optimised SWV method was used to analyse BZP solutions over the concentration range 10 to 60 μM BZP in pH 9.5 BR buffer using the Paste 6 electrode. 500 mL of Pepsi Cola ® was degassed by sonication for 20 min then 20 min nitrogen bubbling. 10.8 mg of BZP hydrochloride was dissolved in 100 mL of the cola and analysed in triplicate using the optimised SWV method. A 3 μM MDMA solution in pH 9.5 BR buffer was analysed by the optimised SWV method in order to assess the selectivity of the method against the most commonly encountered ecstasy-type compound.

3. Results and discussion

3.1. Electrode material determination

The three CVs for the initial scan of BZP are shown in Fig. 4. Platinum did not show any response to BZP that was not also present in the blank

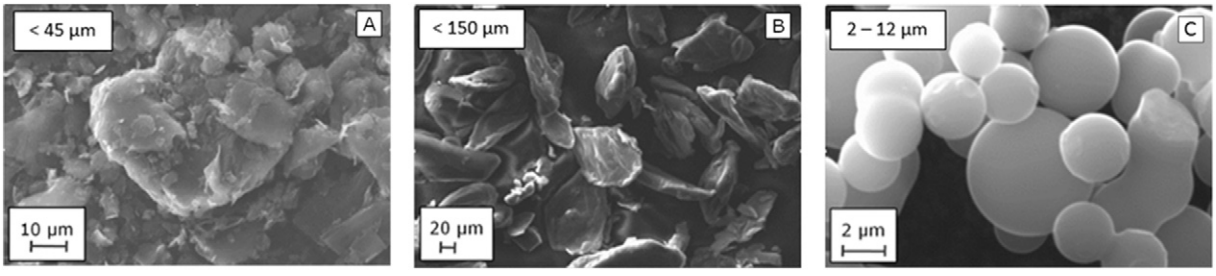

Fig. 5. SEM micrographs of carbon powder. The particle size is shown in the top left of each image and the scale is shown in the bottom left. Image A and B are graphite and image C is glassy carbon.

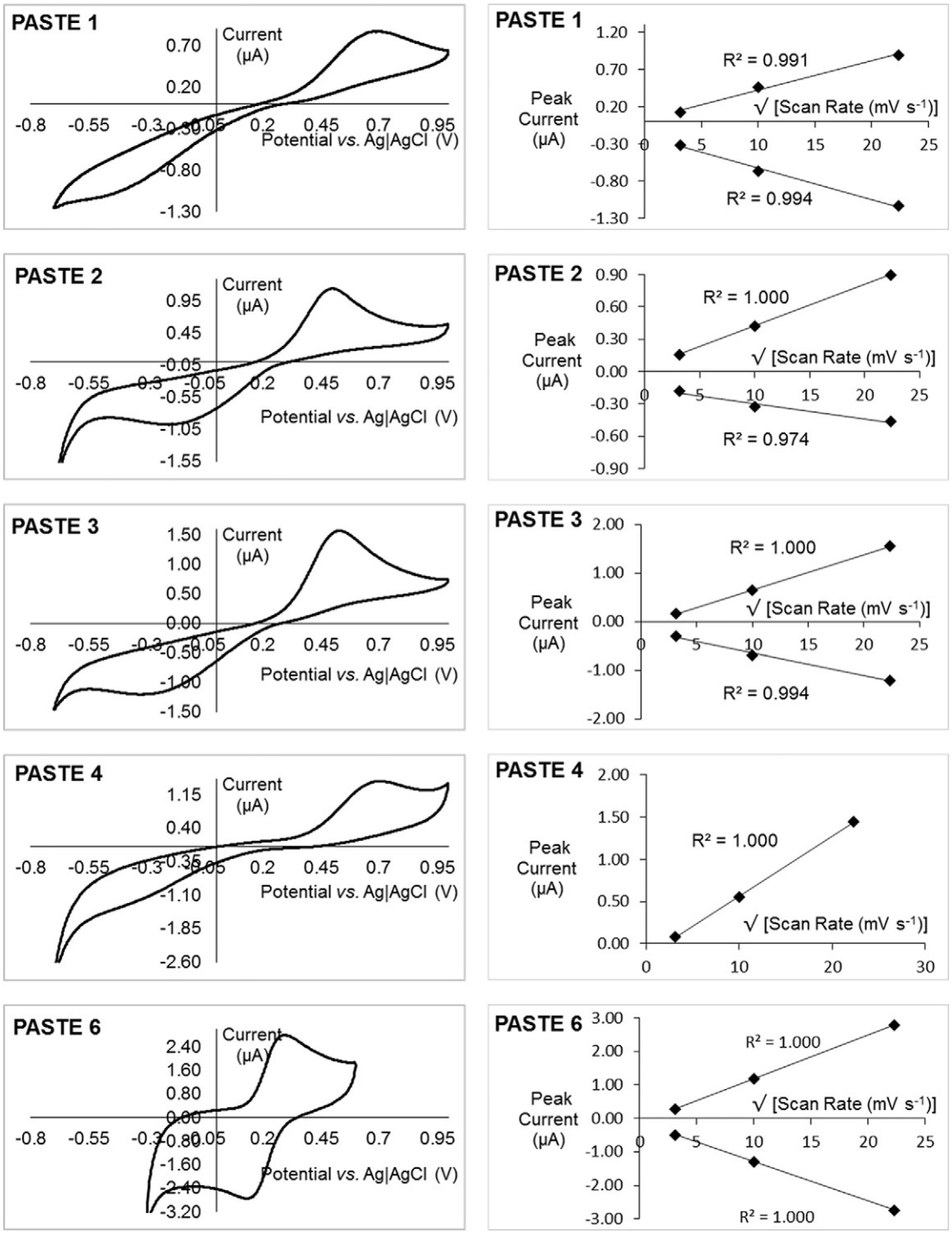

Fig. 6. CVs on the left and corresponding Randles-Sevcik plots on the right for the five functional electrodes using 99 μM $K_3Fe(CN)_6$ in 0.1 M KCl ($\upsilon = 500$ mV s^{-1} in scans shown). The composition for the paste number in the top left of each is given in Table 2.

Table 5
Summary of assessment data for $K_3Fe(CN)_6$ in 0.1 M KCl for the five functional paste electrodes. The CV data in the columns two and three was measured at 99 μM.

Paste number	CV ΔE_p at 100 mV s^{-1} (V)	CV Ratio of slopes from Randles-Sevcik plots	SWV Sensitivity (A M^{-1})	SWV RSD of Peak Potential (%)
1	0.90	1.1	3.69×10^{-4}	1.43
2	0.45	0.4	5.69×10^{-3}	1.18
3	0.55	0.6	2.75×10^{-3}	0.73
4	0.80	No reduction peak observed	2.58×10^{-3}	0.88
6	0.08	0.9	4.79×10^{-2}	0.00

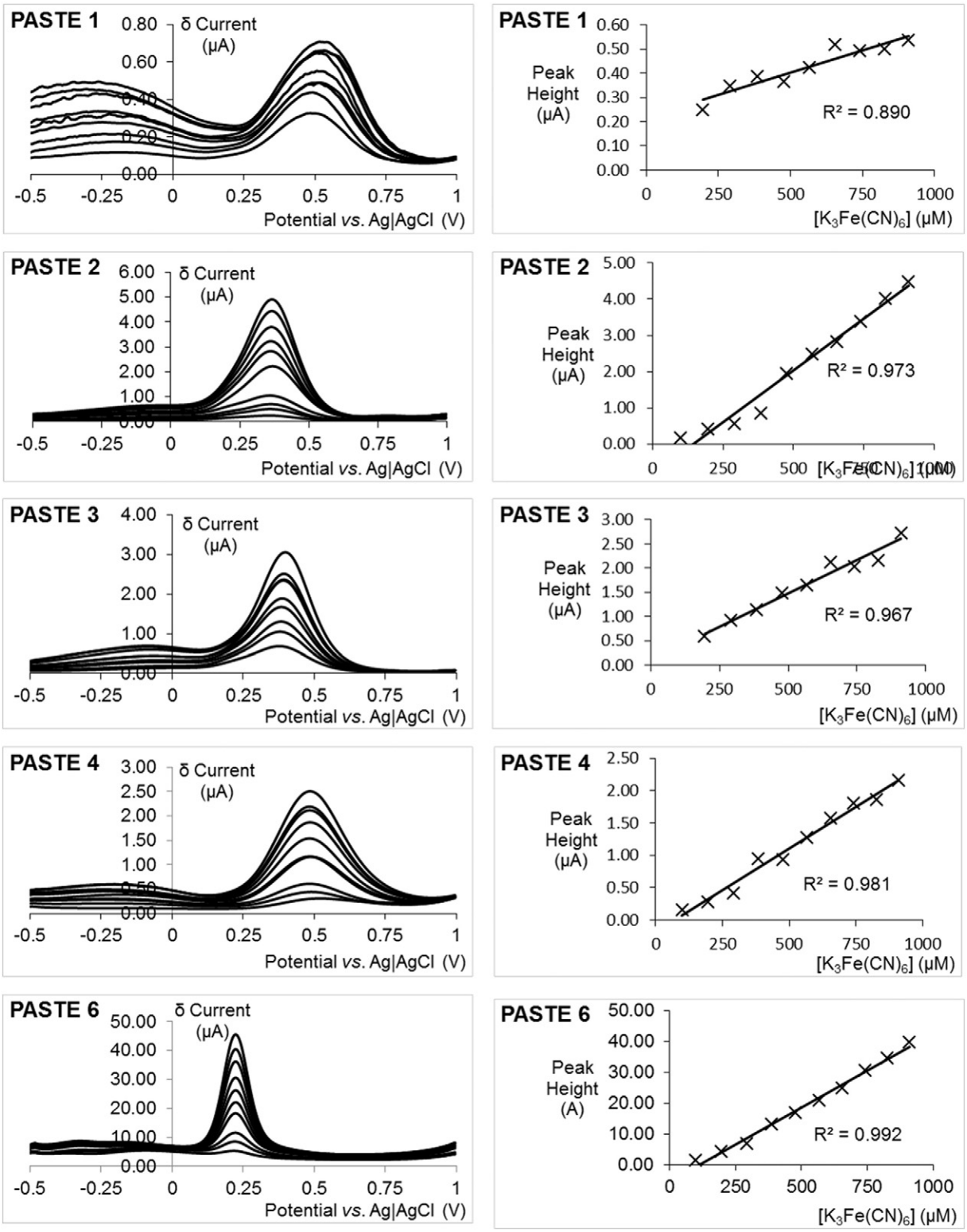

Fig. 7. SWVs on the left and the corresponding regression plots for varying concentrations of $K_3Fe(CN)_6$ in 0.1 M KCl. The composition for the paste number in the top left of each is given in Table 2.

CV so was thus discarded from further investigation. The gold electrode showed a reversible peak which was also present in the blank considered to be formation and removal of an oxide layer. However at approximately 0.8 V a non-reversible oxidative peak was present which corresponded to BZP. This peak was also present in the graphite electrode CV. Due to the response to graphite for BZP being highest of those tested and the general wide applicability of carbon electrodes, it was decided to pursue carbon as the electrode material.

The SEM images of the types of carbon that were investigated are shown in Fig. 5. The two graphite powders had highly irregular morphology but generally were within the particle size listed by the manufacturer (as estimated by the SEM's sizing capability). However the glassy carbon particles were much more regular being almost entirely spherical and again falling within the manufacturer specified size. The six different carbon paste electrodes were then evaluated using $K_3Fe(CN)_6$ as a model compound as it is known to have excellent reversibility characteristics. It was immediately discovered that Paste 5 failed to produce any signal which is assumed to be due to lack of conductivity. The CVs for the five remaining paste electrodes are shown in Fig. 6 alongside the Randles-Sevcik – plots of peak current (I_P) versus the square root of the scan rate – for each paste. The most striking feature from the CVs is that Paste 6 shows by far the most reversible characteristics; the peak to peak separations for Pastes 1 to 4 are all >100 mV even at the slowest scan rate whereas ideally for a reversible single electron transfer such as in the ferricyanide ion 60 mV would be expected. Indeed Paste 6 is the only one to have the cathodic wave in the positive potential region, although it also has the highest background capacitance shown by the vertical distance between the forward and reverse waves. The cathodic Randles-Sevcik plot for Paste 4 was not determined because the peak potential E_{PC} was not distinctly formed against the background wave. The cyclic data for the five functional pastes are summarised in Table 5. As the peak to peak separation (ΔE_P) for Paste 6 is clearly the lowest and the ratio of the slopes for Paste 6′s cathodic and anodic Randles-Sevcik plots is close to 1 it has the best reversibility characteristics. The sensitivity of each of the pastes was also investigated by SWV and the voltammograms alongside the regression curves are shown in Fig. 7. Table 5 also summarises the two important features from the SWV data namely Paste 6 has a sensitivity which is at least an order of magnitude bigger than that of the other pastes and the precision of the peak potential in Paste 6 is impeccable – it was the same value for each concentration. As Paste 6 clearly had the fastest heterogeneous electron transfer, as shown by its reversibility and sensitivity, it was chosen for the subsequent analysis when the focus of the research returned to BZP.

3.2. Mechanism of BZP oxidation

The data for the LSV analysis at varying pH is shown in Fig. 8, however it should be noted that the first differential of the current with respect to the potential has been plotted for clarity. It was noted that E_P decreased with increasing pH according to the relationship E_P (V) $= -0.062 \times$ pH $+ 1.353$ (V) ($R^2 = 0.98$). The closeness of the slope to $^{-}0.059$ V pH $^{-1}$ indicates that an equal number of electrons and protons are involved in the charge transfer mechanism by analogy to the Nernst equation. Other than decaying at either extreme of the pH scale there did not appear to be a clear relationship between I_P and pH. Therefore the pH value of 9.5 was chosen for further analysis which is close to the pKa value of BZP (literature value 9.59 [29]). This pH serves two advantages: a relatively low value of E_P is used meaning there is less chance of also oxidising interfering compounds and a relatively high I_P is maintained. An E_P – pH relationship such as this also indicates that it is the amine group which is being oxidised rather than the aromatic ring. The mechanism was further investigated by altering the scan rates used in LSV and the results of which are shown in Fig. 9, where again the first differential of current with respect to potential has been plotted. This data indicated a diffusion limited process as there was a linear relationship between the square root of the scan rate and the peak current (I_P (A) $= 8.802 \times 10^{-4}$ (υ V s^{-1})$^{-0.5}$ – 1.968×10^{-4} (A), with $R^2 = 0.99$). The peak potential (E_P) was also observed to shift to higher values with increasing scan rate and a linear relationship was observed between the ln υ and E_P (E_P (V) $= 0.0317$ ln (υ V s^{-1}) $+ 0.7665$ (V). In general the shift in peak potential for a completely irreversible process with changing scan rate is given by Eq. (1) [30]:

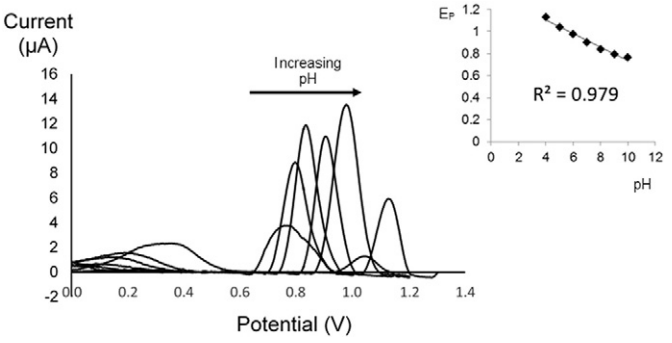

Fig. 8. First differential of LSV analysis of 49 μM $K_3Fe(CN)_6$ at varying pH. Inset shows the regression of line for how Peak Potential (EP) changes with pH (n = 3).

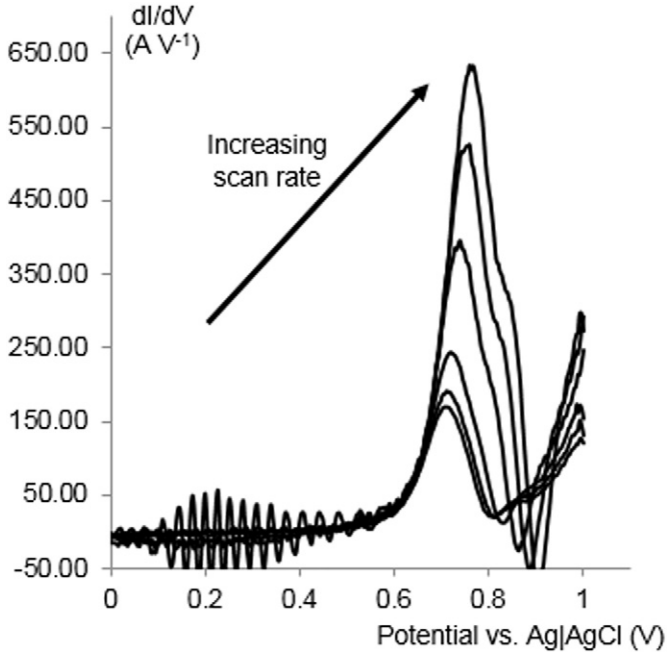

Fig. 9. First differential of LSV analysis of 120 μM $K_3Fe(CN)_6$ at varying scan rate in pH 9 BR buffer (n = 3).

$$E_P = E_f^{\circ} - \frac{RT}{\alpha n F} \ln \frac{RTk^{\circ}}{\alpha n F} + \frac{RT}{\alpha n F} \ln \upsilon \quad (1)$$

where E_f° is the formal potential, R, T and F have their usual assignments, α is the transfer coefficient, n is the number of electrons involved in the charge transfer and k^o is the heterogenous rate constant. Therefore by analogy with the last term in Eq. (1) and the slope of the graph of E_P versus ln υ, the value of αn can be estimated as 0.8. This data taken in its entirety would seem to support an overall mechanism involving the loss of two electrons and two protons. Therefore the proposed mechanism as shown in Fig. 10 is consistent with the oxidation of tripropylamine as described by Portis et al. [31]. This also explains the complete irreversibility as the tertiary amine is lost at the end of the mechanism due to a homogeneous reaction with the solvent.

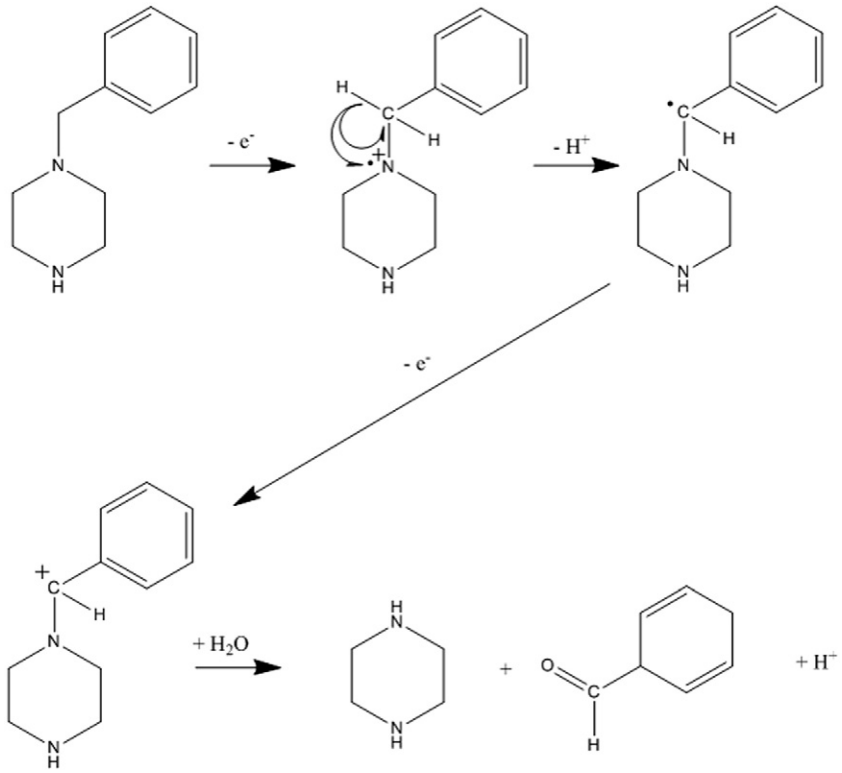

Fig. 10. Proposed two electron and two proton mechanism of BZP oxidation at the carbon paste electrode.

3.3. Optimisation of BZP oxidation at the paste electrode

The attention was then turned to optimising the SWV method for the analysis of BZP. Increasing lengths of time were used for deposition to determine the point at which the electrode would become saturated. The resulting data of peak current versus deposition is shown in Fig. 11. It was obvious that there was no advantage to increasing the deposition time beyond 135 s so this was used for subsequent analysis. A full factorial design was then used to investigate the effects of the SWV parameters: step height, amplitude, and frequency. The results were interpreted both in terms of sensitivity where the absolute value of the peak current was used and in terms of precision where the relative standard deviation of the peak current (n = 3) for each setting was used. It would found that no one factor or combination of factors had a statistically significant effect (at 95% confidence) over the others in terms of sensitivity. However the step height, the frequency and the combination of step height and frequency were found to have a statistically significant effect in terms of precision. Both sensitivity and precision were used in order to find the optimised value for each parameter which was step height 10 mV, amplitude 50 mV and frequency 13 Hz.

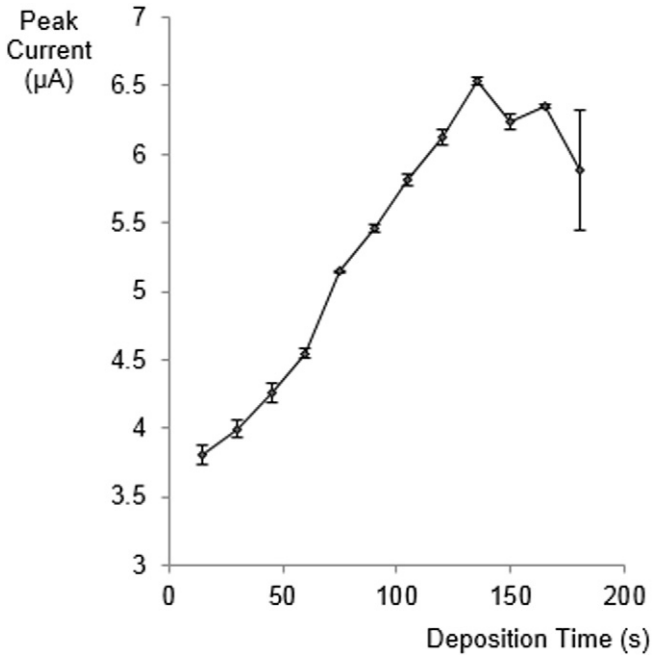

Fig. 11. Investigation of SWV peak current with varying deposition time using the Paste 6 electrode for a 120 μM BZP in pH 9.5 BR buffer. The error bars are 1 standard deviation (n = 3).

3.4. Validation of the optimised method

The validation of the method began with the analysis of range of concentrations of BZP in order to assess linearity and the limit of detection and quantification (LOD and LOQ). The regression data is shown in Fig. 12. The method was shown to be linear between 12 and 68 μM ($R^2 = 0.99$) beyond this range it was noted there was slight deviation, however it was also noted that there was linearity if tested over a higher range e.g. 100 to 200 μM (data not shown). The LOD and LOQ were determined using the sum of the square of the residuals method (i.e. 3 and 10 times the standard deviation of the blank) and were found to be 6 and 20 μM respectively. As an example application a 61 μM BZP in Pepsi Cola solution was tested against a Pepsi Cola blank. The blank did not have any peaks in the region of the BZP oxidation and the concentration was determined by reference to the linear regression used in the LOD determination. A comparison of the concentration by weight and the concentration by calculation showed the values to agree to within 0.08% which was excellent precision (n = 3). Lastly a solution of MDMA was analysed

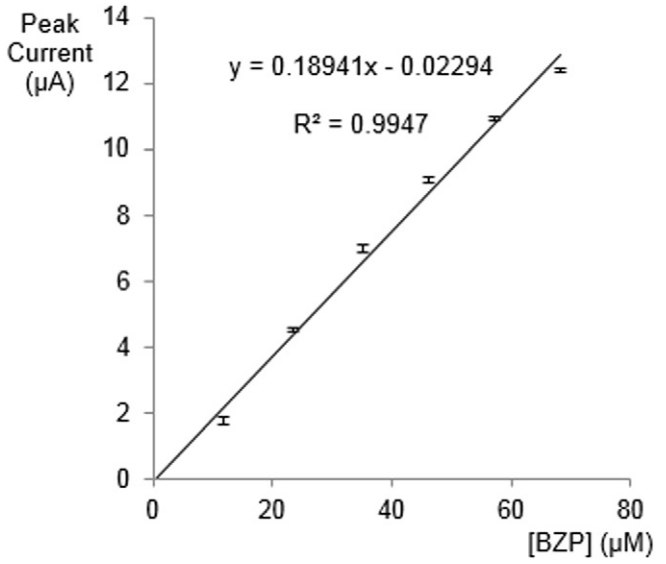

Fig. 12. Regression calibration for BZP using the Paste 6 electrode in pH 9.5 BR buffer and the optimised SWV method. The error bars are 1 standard deviation (n = 3).

using the optimised SWV and a comparison of the voltammograms with BZP is shown in Fig. 13. It was noted that although the peaks were not completely resolved there was a separation of 90 mV and it would be possible to distinguish between them in combination with the analysis of standards. The resolution was found to be 0.45 which was calculated by dividing the difference in peak potential by the average peak width.

4. Conclusion

An analytical method has been developed which offers the promise of portability, cheapness, speed, precision and accuracy for the analysis of BZP. Although there are many analytical techniques which have superior LOD parameters, this becomes irrelevant in the analysis of bulk drugs which is the future goal of this research. An LOQ of 20 μM is more than sufficient considering the average dose of a tablet is between 50 and 200 mg [32]. However if the analysis of body fluids for the presence of BZP using this technique was to be considered it would be important to assess the resolution between the hydroxylated metabolites and the drug itself.

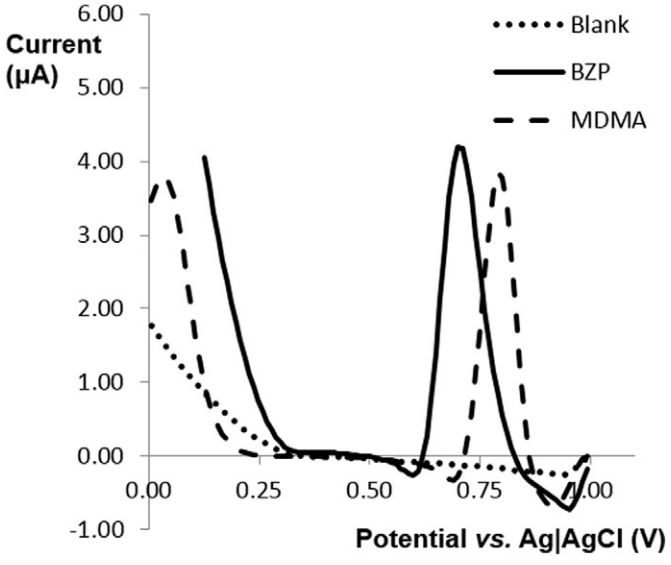

Fig. 13. Optimised SWV comparison using Paste 6 electrode in pH 9.5 BR buffer for 3 μM MDMA and 12 μM BZP for comparison.

Acknowledgements

This research did not receive any specific grant from funding agencies in the public, commercial, or not-for-profit sectors. The authors wish to thank Robert Gordon University for the use of the facilities to conduct the research.

References

[1] T.M. Brunt, R.J.M. Niesink, W. van den Brink, Impact of a transient instability of the ecstasy market on health concerns and drug use patterns in The Netherlands, Int. J. Drug Policy 23 (2) (2012) 134–140.
[2] United Nations Office on Drugs and Crime, World Drug Report, UNODC, Vienna, 2015.
[3] *Psychoactive Substances Act 2016 2016.*
[4] United Nations Office on Drugs and Crime, What are NPS? [homepage on the Internet]. Available from: https://www.unodc.org/LSS/Page/NPS 2016.
[5] J.P. Smith, O.B. Sutcliffe, C.E. BANKS, An overview of recent developments in the analytical detection of new pyschoactive substances (NPSs), Analyst 2015 (140) (2015) 4932–4948.
[6] M.D. Arbo, M.L. Bastos, H.F. Carmo, Piperazine compounds as drugs of abuse, Drug Alcohol Depend. 122 (3) (2012) 174–185.
[7] M. Sá Monteiro, M. de Lourdes Bastos, P.G. de Pinho, M. Carvalho, Update on 1-benzylpiperazine (BZP) part pills, Arch. Toxicol. 87 (2013) 929–947.
[8] EMCDDA, Report on the risk assessment of BZP in the framework of the Council decision on new psychoactive substances, European Monitioring Centre for Drugs and Drug Addiction, 2009.
[9] *Misuse of Drugs Act 1971 (Amendment) Order 2009 2009.*
[10] M. Philp, R. Shimmon, N. Stojanovska, M. Tahtouh, S. Fu, Development and validation of a presumptive colour spot test method for the detection of piperazine analogues in seized illict material, Anal. Methods 5 (20) (2013) 5402–5410.
[11] A.T. Shulgin, D.E. MacLean, Illicit Synthesis of Phencyclidine (PCP) and Several of Its Analogs, Clin. Toxicol. 9 (4) (1976) 553–560.
[12] K. Kovar, M. Laudszun, Chemsitry and reaction mechanisms of rapid tests for drugs of abuse and precursors chemicals, United Nations, Pharmazeutisches Institut der Universität Tübingen, Auf der Morgenstelle 8, D-7400 Tübingen, Federal Republic of Germany, 1989.
[13] L.E. Elie, M.G. Baron, R.S. Croxton, M.P. Elie, Reversing microcrystalline tests—An analytical approach to recycling of microcrystals from drugs of abuse, Forensic Sci. Int. 207 (1–3) (2011) e55–e58.
[14] L. Elie, M. Baron, R. Croxton, M. Elie, Microcrystalline identification of selected designer drugs, Forensic Sci. Int. 214 (1–3) (2012) 182–188.
[15] M.E. Nelson, S.M. Bryant, S.E. Aks, Emerging drugs of abuse, Dis. Mon. 60 (3) (2014) 110–132.
[16] D. de Boer, I.J. Bosman, E. Hidvégi, C. Manzoni, A.A. Benkö, L.J.A.L. dos Reys, et al., Piperazine-like compounds: a new group of designer drugs-of-abuse on the European market, Forensic Sci. Int. 121 (1–2) (2001) 47–56.
[17] M.S. Castaneto, A.J. Barnes, M. Concheiro, K.L. Klette, T.A. Martin, M.A. Huestis, Biochip array technology immunoassay performance and quantitative confirmation of designer piperazines for urine workplace drug testing, Anal. Bioanal. Chem. 407 (16) (2015) 4639–4648.
[18] M.G. Fitzsimons, Y. Ishizawa, K.H. Baker, Drug testing physicians for substances of abuse: case report of a false-positive result, J. Clin. Anesth. 25 (8) (2013) 669–671.
[19] A. Choodum, N. Nic Daeid, Rapid and semi-quantitative presumptive tests for opiate drugs, Talanta 86 (2011) 284–292.
[20] J. Wang, Electrochemical glucose biosensors, Chem. Rev. 108 (2) (2008) 814–825.
[21] P. Kriikku, L. Wilhelm, S. Jenckel, J. Rintatalo, J. Hurme, J. Kramer, et al., Comparison of breath-alcohol screening test results with venous blood alcohol concentration in suspected drunken drivers, Forensic Sci. Int. 239 (0) (2014) 57–61.
[22] P. Skládal, 5 - Electrochemical detection for biological identification, in: R.P. Schaudies (Ed.), Biological Identification, Woodhead Publishing 2014, pp. 131–152.
[23] D. Monticelli, L.M. Laglera, S. Caprara, Miniaturization in voltammetry: Ultratrace element analysis and speciation with twenty-fold sample size reduction, Talanta 128 (0) (2014) 273–277.
[24] R.K. Shervedani, Z. Rezvaninia, H. Sabzyan, H. Zali Boeini, Characterization of gold-thiol-8-hydroxyquinoline self-assembled monolayers for selective recognition of aluminum ion using voltammetry and electrochemical impedance spectroscopy, Anal. Chim. Acta 825 (0) (2014) 34–41.
[25] B. Kaur, R. Srivastava, Simultaneous electrochemical determination of nanomolar concentrations of aminophenol isomers using nanocrystalline zirconosilicate modified carbon paste electrode, Electrochim. Acta 141 (0) (2014) 61–71.
[26] Z. Liu, X. Huang, Voltammetric determination of inorganic arsenic, TrAC Trends Anal. Chem. 60 (0) (2014) 25–35.
[27] J.P. Smith, E.P. Randviir, C.E. Banks, An introduction to Forensic Electrochemistry, in: E. Katz, J. Halámek (Eds.), Forensic Science: A Multidisciplinary Approach, Wiley-VCH, Weinheim, Germany 2016, pp. 89–102.
[28] A.J. Bandodkar, A.M. O'Mahony, J. Ramirez, I.A. Samek, S.M. Anderson, J.R. Windmiller, et al. Solid-state Forensic Finger sensor for integrated sampling and detection of gunshot residue and explosives: towards 'Lab-on-a-finger'. Analyst (18): 5288-5295.

[29] S.C. Bishop, B.R. McCord, S.R. Gratz, J.R. Loeligner, M.R. Witkowski, Simultaneous separation of different types of amphetamine and piperazine designer drugs by capillary electrophoresis with a chiral selector, J. Forensic Sci. 50 (2) (2005) 325–335.
[30] J.P. Smith, J.P. Metters, C. Irving, O.B. Sutcliffe, C.E. Banks, Forensic electrochemistry: the electroanalytical sensing of synthetic cathinone-derivatives and their accompanying adulterants in legal high products, Analyst 139 (2) (2014) 389–400.
[31] L.C. Portis, J.T. Klug, C.K. Mann, Electrochemical Oxidation of Some Phenethylamines, J. Org. Chem. 39 (24) (1974) 3488–3494.
[32] B.M.Z. Cohen, R. Butler, BZP-party pills: A review of research on benzylpiperazine as a recreational drug, Int. J. Drug Policy 22 (2) (2011) 95–101.
[33] H. Tsutsumi, M. Katagi, A. Miki, N. Shima, T. Kamata, M. Nishikawa, et al., Development of simultaneous gas chromatography–mass spectrometric and liquid chromatography–electrospray ionization mass spectrometric determination method for the new designer drugs, N-benzylpiperazine (BZP), 1-(3-trifluoromethylphenyl)piperazine (TFMPP) and their main metabolites in urine, J. Chromatogr. B 819 (2) (2005) 315–322.
[34] M. Takahashi, M. Nagashima, J. Suzuki, T. Seto, I. Yasuda, T. Yoshida, Creation and application of psychoactive designer drugs data library using liquid chromatography with photodiode array spectrophotometry detector and gas chromatography–mass spectrometry, Talanta 77 (4) (2009) 1245–1272.
[35] U. Antia, M.D. Tingle, B.R. Russell, Validation of an LC-MS Method for the Detection and Quantification of BZP and TFMPP and their Hydroxylated Metabolites in Human Plasma and its Application to the Pharmacokinetic Study of TFMPP in Humans*, J. Forensic Sci. 55 (5) (2010) 1311–1318.
[36] A. Wohlfarth, W. Weinmann, S. Dresen, LC-MS/MS screening method for desinger amphetamines, tryptamines, and piperazines, Anal. Bioanal. Chem. 396 (7) (2010) 2403–2414.
[37] C. Chen, C. Kostakis, R.J. Irvine, J.M. White, Increases in use of novel synthetic stimulant are not directly linked to decreased use of 3,4-methylenedioxy-N-methylamphetamine (MDMA), Forensic Sci. Int. 231 (1–3) (2013) 278–283.
[38] Y. Boumrah, M. Rosset, Y. Lecompte, S. Bouanani, K. Khimeche, A. Dahmani, Development of a targeted GC/MS screening method and validation of an HPLC/DAD quantification method for piperazines–amphetamines mixtures in seized material, Egypt. J. Forensic Sci. 4 (3) (2014) 90–99.
[39] A.J. Dickson, S.P. Vorce, J.M. Holler, T.P. Lyons, Detection of 1-Benzylpiperazine, 1-(3-Trifluoromethylphenyl)-piperazine, and 1-(3-Chlorophenyl)-piperazine in 3,4-Methylenedioxymethamphetamine-Positive Urine Samples, J. Anal. Toxicol. 34 (2010) 464–469.
[40] M. Concheiro, M. Castaneto, R. Kronstrand, M.A. Huestis, Simultaneous determination of 40 novel psychoactive stimulants in urine by liquid chromatography–high resolution mass spectrometry and library matching, J. Chromatogr. A 1397 (2015) 32–42.
[41] S. Strano-Rossi, S. Odoardi, M. Fisichella, L. Anzillotti, R. Gottardo, F. Tagliaro, Screening for new psychoactive substances in hair by ultrahigh performance liquid chromatography–electrospray ionization tandem mass spectrometry, J. Chromatogr. A 1372 (2014) 145–156.
[42] N.M. Beckett, S.L. Cresswell, D.I. Grice, J.F. Carter, Isotopic profiling of seized benzylpiperazine and trifluoromethylphenylpiperazine tablets using δ13C and δ15N stable isotopes, Sci. Justice 55 (1) (2015) 51–56.
[43] C. Kuleya, S. Hall, L. Gautam, M.D. Cole, An optimised gas chromatographic-mass spectrometric method for the chemical characterisation of benzylpiperazine and 1-arylpiperazine based drugs, The Royal Society of Chemistry, 2014.
[44] E.M. Mwenesongole, L. Gautam, S.W. Hall, J.W. Waterhouse, M.D. Cole, Simultaneous detection of controlled substances in waste water, The Royal Society of Chemistry, 2013.
[45] A. Niazi, J. Ghasemi, M. Zendehdel, Simultaneous voltammetric determination of morphine and noscapine by adsorptive differential pulse stripping method and least-squares support vector machines, Talanta 74 (2) (2007) 247–254.
[46] F. Li, J. Song, D. Gao, Q. Zhang, D. Han, L. Niu, Simple and rapid voltammetric determination of morphine at electrochemically pretreated glassy carbon electrodes, Talanta 79 (3) (2009) 845–850.
[47] C. Macedo, P.S. Branco, L.M. Ferreira, A.M. Lobo, J.P. Capela, E. Fernandes, et al., Synthesis and Cyclic Voltammetry Studies of 3,4-Methylenedioxymethylamphetamine (MDMA) Human Metabolites, J. Health Sci. 53 (1) (2007) 31–42.
[48] É.N. Oiye, NBd Figueiredo, JFd Andrade, H.M. Tristão, MFd Oliveira, Voltammetric determination of cocaine in confiscated samples using a cobalt hexacyanoferrate film-modified electrode, Forensic Sci. Int. 192 (1–3) (2009) 94–97.
[49] S. Yılmaz, Adsorptive stripping voltammetric determination of zopiclone in tablet dosage forms and human urine, Colloids Surf. B: Biointerfaces 71 (1) (2009) 79–83.
[50] L.M. de Carvalho, D. Correia, S.C. Garcia, A.V. de Bairros, PCd Nascimento, D. Bohrer, A new method for the simultaneous determination of 1,4-benzodiazepines and amfepramone as adulterants in phytotherapeutic formulations by voltammetry, Forensic Sci. Int. 202 (1–3) (2010) 75–81.
[51] E.M.P.J. Garrido, J.M.P.J. Garrido, N. Milhazes, F. Borges, A.M. Oliveira-Brett, Electrochemical oxidation of amphetamine-like drugs and application to electroanalysis of ecstasy in human serum, Bioelectrochemistry 79 (1) (2010) 77–83.
[52] K. Tang, L. Liu, Y. Hong, J. Hu, J. Zhang, C. Cao, Fabrication of indium tin oxides (ITO)-supported poly(3,4-ethylenedioxythiophene) electrodes coated with active IrO2 layer for morphine electrooxidation, J. Appl. Electrochem. 40 (9) (2010) 1699–1704.
[53] Y. Du, C. Chen, J. Yin, B. Li, M. Zhou, S. Dong, et al., Solid-State Probe Based Electrochemical Aptasensor for Cocaine: A Potentially Convenient, Sensitive, Repeatable, and Integrated Sensing Platform for Drugs, Anal. Chem. 82 (4) (2010) 1556–1563.
[54] A. Ensafi, B. Rezaei, H. Krimi-Maleh, An ionic liquid-type multiwall carbon nanotubes paste electrode for electrochemical investigation and determination of morphine, Ionics 17 (7) (2011) 659–668.
[55] G. Yang, Y. Chen, L. Li, Y. Yang, Direct electrochemical determination of morphine on a novel gold nanotube arrays electrode, Clin. Chim. Acta 412 (17–18) (2011) 1544–1549.
[56] Y. Wen, H. Pei, Y. Wan, Y. Su, Q. Huang, S. Song, et al., DNA Nanostructure-Decorated Surfaces for Enhanced Aptamer-Target Binding and Electrochemical Cocaine Sensors, Anal. Chem. 83 (19) (2011) 7418–7423.
[57] A. Câmpean, M. Tertiș, R. Săndulescu, Voltammetric determination of some alkaloids and other compounds in pharmaceuticals and urine using an electrochemically activated glassy carbon electrode, Cent. Eur. J. Chem. 9 (4) (2011) 688–700.
[58] N.F. Atta, A. Galal, A.A. Wassel, A.H. Ibrahim, Sensitive Electrochemical Determination of Morphine Using Gold-Nanoparticles-Ferrocene Modified Carbon Paste Electrode, Int. J. Electrochem. Sci. 7 (2012) 10501–10518.
[59] A.A. Ensafi, M. Izadi, B. Rezaei, H. Karimi-Maleh, N-hexyl-3-methylimidazolium hexafluoro phosphate/multiwall carbon nanotubes paste electrode as a biosensor for voltammetric detection of morphine, J. Mol. Liq. 174 (0) (2012) 42–47.
[60] M.A. Balbino, M.M.T. de Menezes, I.C. Eleotério, A.A. Saczk, L.L. Okumura, H.M. Tristão, et al., Voltammetric determination of Δ9-THC in glassy carbon electrode: An important contribution to forensic electroanalysis, Forensic Sci. Int. 221 (1–3) (2012) 29–32.
[61] M. Reza Shishehbore, H.R. Zare, D. Nematollahi, Electrocatalytic determination of morphine at the surface of a carbon paste electrode spiked with a hydroquinone derivative and carbon nanotubes, J. Electroanal. Chem. 665 (0) (2012) 45–51.
[62] A. Navaee, A. Salimi, H. Teymourian, Graphene nanosheets modified glassy carbon electrode for simultaneous detection of heroine, morphine and noscapine, Biosens. Bioelectron. 31 (1) (2012) 205–211.
[63] Y. Hong, J. Hu, J. Zhang, C. Cao, Enhanced Electrocatalytic Activity for Morphine Oxidation at 2-Aminoethanethiol Self-Assembled Monolayer (SAM)-Modified Gold Electrode, Electrocatalysis 4 (4) (2013) 302–305.
[64] V. Arabali, R. Sadeghi, Surface properties of nano-Al2O3 film and its application in the preparation of morphine electrochemical sensor, Ionics 19 (12) (2013) 1775–1782.
[65] R. Jiménez-Pérez, J.M. Sevilla, T. Pineda, M. Blázquez, J. González-Rodríguez, Electrochemical behaviour of gamma hydroxybutyric acid at a platinum electrode in acidic medium, Electrochim. Acta 111 (0) (2013) 601–607.
[66] Y. Li, K. Li, G. Song, J. Liu, K. Zhang, B. Ye, Electrochemical behavior of codeine and its sensitive determination on graphene-based modified electrode, Sensors Actuators B Chem. 182 (0) (2013) 401–407.
[67] L.S. de Oliveira, M.A. Balbino, M.M.T. de Menezes, E.R. Dockal, M.F. de Oliveira, Voltammetric analysis of cocaine using platinum and glassy carbon electrodes chemically modified with Uranyl Schiff base films, Microchem. J. (April 26 2013) (accepted for publication).
[68] M. Behpour, A. Valipour, M. Keshavarz, Determination of buprenorphine by differential pulse voltammetry on carbon paste electrode using SDS as an enhancement factor, Mater. Sci. Eng. C 42 (0) (2014) 500–505.
[69] A.L. Sanati, H. Karimi-Maleh, A. Badiei, P. Biparva, A.A. Ensafi, A voltammetric sensor based on NiO/CNTs ionic liquid carbon paste electrode for determination of morphine in the presence of diclofenac, Mater. Sci. Eng. C 35 (0) (2014) 379–385.
[70] Y. Li, L. Zou, Y. Li, K. Li, B. Ye, A new voltammetric sensor for morphine detection based on electrochemically reduced MWNTs-doped graphene oxide composite film, Sensors Actuators B Chem. 201 (0) (2014) 511–519.
[71] H. Ahmar, H. Tabani, M. Hossein Koruni, S.S.H. Davarani, A.R. Fakhari, A new platform for sensing urinary morphine based on carrier assisted electromembrane extraction followed by adsorptive stripping voltammetric detection on screen-printed electrode, Biosens. Bioelectron. 54 (0) (2014) 189–194.
[72] A. Afkhami, F. Soltani-Felehgari, T. Madrakian, A sensitive electrochemical sensor for rapid determination of methadone in biological fluids using carbon paste electrode modified with gold nanofilm, Talanta 128 (0) (2014) 203–210.
[73] M.C. Tadini, M.A. Balbino, I.C. Eleoterio, L.S. de Oliveira, L.G. Dias, G. Jean-François Demets, et al., Developing electrodes chemically modified with cucurbit[6]uril to detect 3,4-methylenedioxymethamphetamine (MDMA) by voltammetry, Electrochim. Acta 121 (0) (2014) 188–193.
[74] B. Nigović, M. Sadiković, M. Sertić, Multi-walled carbon nanotubes/Nafion composite film modified electrode as a sensor for simultaneous determination of ondansetron and morphine, Talanta 122 (0) (2014) 187–194.
[75] A.A. Ensafi, E. Heydari-Bafrooei, B. Rezaei, Different interaction of codeine and morphine with DNA: A concept for simultaneous determination, Biosens. Bioelectron. 41 (0) (2013) 627–633.